

A Two-Stage Approach to Estimate the Angles of Arrival and the Angular Spreads of Locally Scattered Sources

Mehrez Souden, *Student Member, IEEE*, Sofiène Affes, *Senior Member, IEEE*, and Jacob Benesty, *Senior Member, IEEE*

Abstract—We propose a new two-stage approach to estimate the nominal angles of arrival (AoAs) and the angular spreads (ASs) of multiple locally scattered sources using a uniform linear array (ULA) of sensors. In contrast to earlier works, we consider both long- and short-term channel variations, typically encountered in wireless links. In the first stage, we exploit sources independence to blindly estimate the channel over several data blocks regularly spaced by intervals larger than the coherence time but each, short enough in length, to make time variations negligible within the block duration. We, thereby, decouple the multisource channel parameters estimation problem in hand into parallel and independent single-source channel parameters estimation subproblems. In the second stage, for each spatially scattered source, we process the corresponding sequence of quasi-independent channel realization estimates as a new single-scattered-source observation over which we apply Taylor series expansions to transform the estimation of the nominal AoA and the AS of the corresponding scattered source into a simple localization of two closely spaced, equi-powered, and uncorrelated rays (i.e., point sources). To localize both rays, we propose new accurate and computationally simple closed-form expressions for the mean value of the spatial harmonics and their separation by means of covariance fitting. An asymptotic performance analysis is also provided to prove the efficiency of the proposed estimators. Then, the AS and the nominal AoA of every source are directly deduced. The whole proposed framework takes advantage of the capabilities of the preprocessing channel identification step (to reduce the noise effect and decouple the estimation of the channel parameters of every source from the others) and the new simple and accurate closed-form estimators to accurately retrieve the channel parameters even in the most adverse conditions, mainly low signal-to-noise ratio (SNR), few sensors, no prior knowledge of the angular distribution, and closely spaced sources, as supported by simulations.

Index Terms—Angular spread, closely spaced sources, locally scattered sources, long/short term wireless channel variations, nominal angle of arrival, source localization.

Manuscript received January 22, 2007; revised August 21, 2007. This work was supported in part by a Canada Research Chair in High-Speed Wireless Communications and by the Strategic Partnership Grants Program of NSERC. The associate editor coordinating the review of this manuscript and approving it for publication was Dr. Jan C. de Munck.

The authors are with the INRS-ÉMT, Université du Québec, Montréal, QC, H5A 1K6 Canada (e-mail: souden@emt.inrs.ca; affes@emt.inrs.ca; benesty@emt.inrs.ca).

Color versions of one or more of the figures in this paper are available online at <http://ieeexplore.ieee.org>.

Digital Object Identifier 10.1109/TSP.2007.909223

I. INTRODUCTION

IN mobile communication systems, the performance of source localization algorithms is largely affected by the multipath phenomenon. Indeed, on the uplink, the energy transmitted by a single source (mobile terminal) reaches the receiver within a cluster of rays after bouncing from several surrounding scatterers. This phenomenon has a negative impact on classical localization algorithms since the point source assumption no longer holds [1]. In such context, the nominal angles of arrival (AoAs) and the angular spreads (ASs) (defined as the standard deviation of angular deviation around the nominal AoA of a scattered source) are critical parameters in the design of SDMA systems [2], [3], source localizers [4], and detectors [5].

Local scattering models have been recently investigated in several works including [1]–[11]. Such models are of particular interest in suburban areas and macro-cell environments where scattering is caused by reflectors around the mobile terminals while the base stations are usually deployed far from scattering. In [2], [12], and references therein, it has been specified that the AS values encountered in macro-cell environments are typically lower than ten degrees. This fact is desirable since it justifies the recourse to Taylor series expansions to alleviate the complexity of estimating channel parameters. In contrast to some computationally complex approaches such as the maximum likelihood (ML) [6], the dispersed signal parameter estimator (DISPARE) [7], and the covariance fitting [11], a notable simplification has been provided in [8]. Therein, the estimation of the AS and the nominal AoA of a scattered source has been transformed into the localization of two rays symmetrically positioned around the nominal AoA. Subsequently, a classical localization algorithm has been used to estimate both “virtual” AoAs and deduce the required parameters. The focus in [8] has been on root-MUSIC [13] which was shown to provide better accuracy with relatively low computational complexity compared to some other point-source localization algorithms [14], [15]. Nevertheless, it has been established that the performance of such algorithm (which is a polynomial version of the spectral MUSIC [16]) deteriorates as the angular separation between the sources of interest decreases [17], [18]. This fact becomes more significant when few sensors are deployed. Hence, the utilization of this algorithm to localize both rays (corresponding to a single spread source) in this context is somehow inappropriate in practical situations where the receiving end is equipped with few sensors due to space or cost constraints. In the case of multiple spread sources, spatial spacing between sources has a key

effect on ASs and nominal AoAs estimation, as it can be directly seen when approximating each scattered source by two virtual rays [8]. Indeed, when the angular separation between two spread sources decreases, their corresponding virtual rays become closer and the resulting covariance matrix conditioning deteriorates leading to severe degradation of the channel parameters estimation accuracy.

To model the multipath propagation in the aforementioned environments, it is commonly assumed that the received signals result from the superposition of a very large number of identically distributed and uncorrelated (or more restrictively independent) frontwaves originating from every transmitting source [8]. This feature is termed as “incoherent source distribution.” In practical applications, the wireless channel has a certain coherence time and can be considered as static within relatively small observation windows. This situation is plausible and has been commonly exploited in several applications including blind and pilot-signals-based channel estimation algorithms (at least during the estimation process) [19]–[24], etc., and to investigate the effect of local scattering on MUSIC [16] in [1]. On the other hand, earlier works [4]–[11] focusing on locally scattered sources’ ASs and nominal AoAs estimation supposed that the channel varies at a fast rate (in some references, e.g., [6], the channel is assumed to vary from one snapshot to another). To meet such an assumption, one might choose the sampling period larger than the channel coherence time. In fact, with an appropriate selection of the sampling instants, both slow and fast time variations can be exploited to enhance parameters estimation in the case of multiple locally scattered sources, as we show in this contribution.

This work is motivated by the need to develop a new simple and accurate technique that estimates the ASs and the nominal AoAs of multiple locally scattered sources even in adverse conditions [low signal-to-noise ratio (SNR), few sensors, no prior knowledge of the angular distribution, and closely spaced sources]. To this end, we propose a new two-stage approach to decouple the general problem in hand into independent and parallel single-source channel parameters estimation subproblems. This decoupling is achieved by adding a blind channel identification preprocessing stage which is performed over several data blocks regularly spaced by intervals larger than the coherence time but each, short enough in length, to make time variations negligible within the block duration. In a second stage, for each spread source, we process the corresponding sequence of channel realization estimates as a new single-scattered-source observation over which we apply Taylor series expansions to transform the estimation of the nominal AoA and the AS of the corresponding scattered source into the localization of two closely spaced point sources as it has been suggested in [8]. To localize both rays, we propose new simple and accurate closed-form estimators of the mean value of the spatial harmonics and their separation by means of covariance fitting. An asymptotic performance of these estimators is also proposed. Finally, we directly retrieve the AS and the nominal AoA of every source.

This paper is organized as follows. In Section II, we present a thorough statement of the problem in hand including the data model, the assumptions, and a description of the short and long-term (or slow/fast) wireless channel behavior. In Section III, we

investigate the blind channel estimation preprocessing stage. In Section IV, we briefly review the Taylor series approximations that have been commonly used in the context of local scattering. We also provide some details about the two-ray approximate data model developed in [8]. In Section V, we detail the new localization algorithm that applies for the case of two equi-powered point sources and present a theoretical investigation of its performance. In Section VI, we present several numerical examples to illustrate the efficiency of the proposed approach. In Section VII, we draw out some concluding remarks.

II. PROBLEM STATEMENT AND ASSUMPTIONS

We suppose N narrowband, stationary, ergodic, independent, and non-Gaussian sources. Each source is scattered by a large number of scatterers within its vicinity to generate L wavefronts. This scenario is practical in the radio communications context where every source models a mobile terminal surrounded by scatterers [12], [25]. At instant t , the considered sources, represented by an N -dimensional vector $\mathbf{s}(t) = [s_1(t) \cdots s_N(t)]^T$, impinge on M sensors yielding an M -dimensional observation vector $\mathbf{x}(t) = [x_1(t) \cdots x_M(t)]^T$. The channel is then modeled as an $M \times N$ matrix $\mathbf{H}(t)$, and $\mathbf{x}(t)$ is expressed as

$$\mathbf{x}(t) = \mathbf{H}(t) \mathbf{s}(t) + \mathbf{b}(t) \quad (1)$$

where $\mathbf{b}(t) = [b_1(t) \cdots b_M(t)]^T$ is an unknown noise vector composed of M Gaussian i.i.d. zero-mean stationary signals independent of the sources and with variance σ_b^2 . The L wavefronts generated from the n th source are impinging from different directions $(\tilde{\theta}_{nl})_{1 \leq l \leq L}$, assumed to be symmetrically distributed around the nominal AoA, θ_n , on the sensors array. Hence, the n th channel matrix column is expressed as [1]–[11]

$$\mathbf{h}_n(t) = \sum_{l=1}^L \gamma_{nl}(t) \mathbf{a}[\theta_n(t) + \tilde{\theta}_{nl}(t)] \quad (2)$$

where \mathbf{a} represents the steering vector whose expression strongly depends on the geometry of the sensors array. In this paper, we consider only the case of a ULA. Hence, $\mathbf{a}(\theta)$ is expressed as

$$\mathbf{a}(\theta) = \left[1 \ e^{j2\pi\kappa \sin(\theta)} \ \dots \ e^{j2(M-1)\pi\kappa \sin(\theta)} \right]^T \quad (3)$$

where κ is the sensors separation in wavelengths, and $(\cdot)^T$ denotes the transpose operator. Typically, we have $\kappa = 1/2$. Fig. 1 is an illustration of the data model in presence of two sources. In the case of an incoherent source distribution with Rayleigh fading (for a large number of scatterers), the channel gains $(\gamma_{nl})_{1 \leq l \leq L}$ are assumed to be uncorrelated, zero-mean complex Gaussian random variables. Actually, γ_{nl} and $\tilde{\theta}_{nl}$ fully characterize the l th wavefront generated from the n th source, and are the realizations of the stochastic processes γ_n and $\tilde{\theta}_n$, respectively. We also assume as in [8] that $\tilde{\theta}_n$ is zero-mean and symmetrically distributed with small standard deviation. As stated earlier, this hypothesis is practical in macrocell environments. Eventually, we suppose that the nominal AoAs

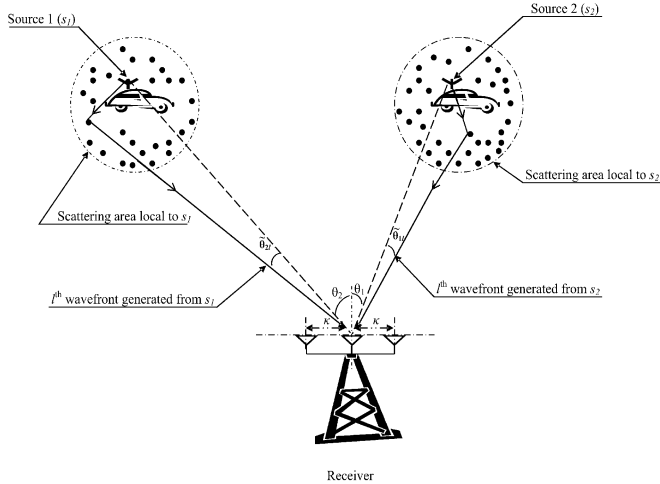


Fig. 1. An illustration of the local scattering model; case of two sources and a ULA of three sensors at the receiver.

$(\theta_n)_{1 \leq n \leq N}$ are invariant (time-independent) in all our processing, as in [1]–[11]. The latter assumption is plausible if we suppose that the sources are sufficiently far from the receiver and slowly moving as in the radio communication environments. Our objective in this paper is to estimate $(\theta_n)_{1 \leq n \leq N}$ and the ASs $(\sigma_{\theta_n})_{1 \leq n \leq N}$ which are the standard deviations of $(\tilde{\theta}_n)_{1 \leq n \leq N}$.

In several situations, the mobile terminal's speed is low leading the wireless channel spatial properties to be slowly changing. In other words, the random variables $\tilde{\theta}_n$ and γ_n are slowly varying. In the bottom of Fig. 2, we see that within a short data block, the ray's magnitude can be assumed as constant. The same slow variations behavior is observed with the other parameters characterizing the ray. This special feature of the channel has been exploited in several works including [19]–[24], etc. On the other hand, the channel remarkably changes between two distant-enough blocks (i.e., when separated by durations larger than the coherence time). In what follows, we will use T_c , T' , T , and K to denote the channel coherence time, the data blocks separation, the length of each data block, and the total number of data blocks, respectively. Note that all these quantities are normalized by the sampling period. The overall number of snapshots will be denoted $T_w = KT$. In order to have the channel time variations negligible within each block duration but independent between each two consecutive data blocks, the following condition should be satisfied:

$$T \leq T_c < T'. \quad (4)$$

In this paper, we take advantage of both aspects of short/long-term channel variations. Indeed, we first estimate the channel over K T -length data blocks. Then, we combine all the estimates to retrieve the ASs and the AoAs as illustrated in Fig. 2 and explained later.

III. PREPROCESSING: BLIND CHANNEL IDENTIFICATION

Since the sources are independent, we use blind channel identification (through independent component analysis) as a pre-

processing step in order to decouple the multisource channel parameters (ASs and nominal AoAs) estimation problem into N independent and parallel subproblems. Hence, the performance of the proposed method strongly depends on this stage. Precisely, a fast convergent and accurate channel estimation algorithm is required to have less computational complexity and acceptable accuracy with a limited number of snapshots. A comparison of different blind channel identification (or equivalently blind source separation) techniques can be found in [26]. This preprocessing step has two main advantages: i) it transforms the general multisource problem in hand into the estimation of the AS and nominal AoA of every source separately, and ii) in case of colored Gaussian noise, the channel realizations can be estimated using fourth-order statistics [20], rendering the estimation of the ASs and the AoAs by the second stage possible in such a case, in contrast with previous techniques.

We run the blind channel identification algorithm that will be noted BCI in the sequel over each of the K blocks (cf. Fig. 2). The K channel matrix realizations are blindly estimated up to some scale and permutation indeterminacies for the K data blocks. In other words, performing BCI over the T observations of the k th data block forming the matrix $\mathbf{X}(k) \triangleq [\mathbf{x}(kT') + 1] \dots \mathbf{x}(kT' + T)$ leads to the following estimate of the channel matrix [21], [22]:

$$\hat{\mathbf{H}}(k) = \mathbf{H}(k)\mathcal{P}(k)\mathbf{D}(k) + \mathbf{E}(k) \quad (5)$$

where $\mathbf{D}(k) = \text{diag}[\alpha_1(k) \dots \alpha_N(k)]$ is a diagonal matrix composed of scalar indeterminacies, $\mathcal{P}(k)$ is a permutation matrix, and $\mathbf{E}(k)$ is an "error matrix" representing the estimation residue of this preprocessing step.

A. Covariance Matrix and Practical Considerations

Here, we suppose that the permutation indeterminacies are solved in $\hat{\mathbf{H}}(k)$ defined in (5) leading to $\hat{\mathbf{H}}(k) = \hat{\mathbf{H}}(k)\mathbf{P}^T(k)$ where $\mathbf{P}(k)$ is a permutation matrix relative to the first channel estimate [$\mathbf{P}(0) = \mathbf{I}_N$]. We will address this issue in the following subsection. The n th column of the channel matrix has K realizations $[\mathbf{h}_n(k)]_{0 \leq k \leq K-1}$ whose estimates are

$$\begin{aligned} \hat{\mathbf{h}}_n(k) &= \alpha_n(k)\mathbf{h}_n(k) + \mathbf{e}_n(k) \\ &= \alpha_n(k) \sum_{l=1}^L \gamma_{nl}(k)\mathbf{a}[\theta_n + \tilde{\theta}_{nl}(k)] + \mathbf{e}_n(k) \end{aligned} \quad (6)$$

where $\mathbf{e}_n(k)$ and $\hat{\mathbf{h}}_n(k)$ are the n th column vectors of $\mathbf{E}(k)$ defined in (5) and $\hat{\mathbf{H}}(k)$, respectively. Notice here that (6) has the same form as the data model that has been considered in the literature to estimate the AS and the nominal AoA in the case of a single scattered source [1], [2], [6], [8]. Furthermore, the assumption of incoherently distributed sources with random channel realizations is now satisfied provided that the K data blocks are enough spaced (by intervals larger than the channel's coherence time) such that for $n \in \{1, \dots, N\}$, $[\gamma_{nl}(k)]_{0 \leq k \leq K-1}$ models a sequence of realizations of a random variable which is uncorrelated with $[\gamma_{n'l'}(k)]_{0 \leq k \leq K-1} \forall l, l' \in \{1, \dots, L\}$ such that $l \neq l'$. The scale indeterminacies $[\alpha_n(k)]_{0 \leq k \leq K-1}$ have no effect as it will be demonstrated later

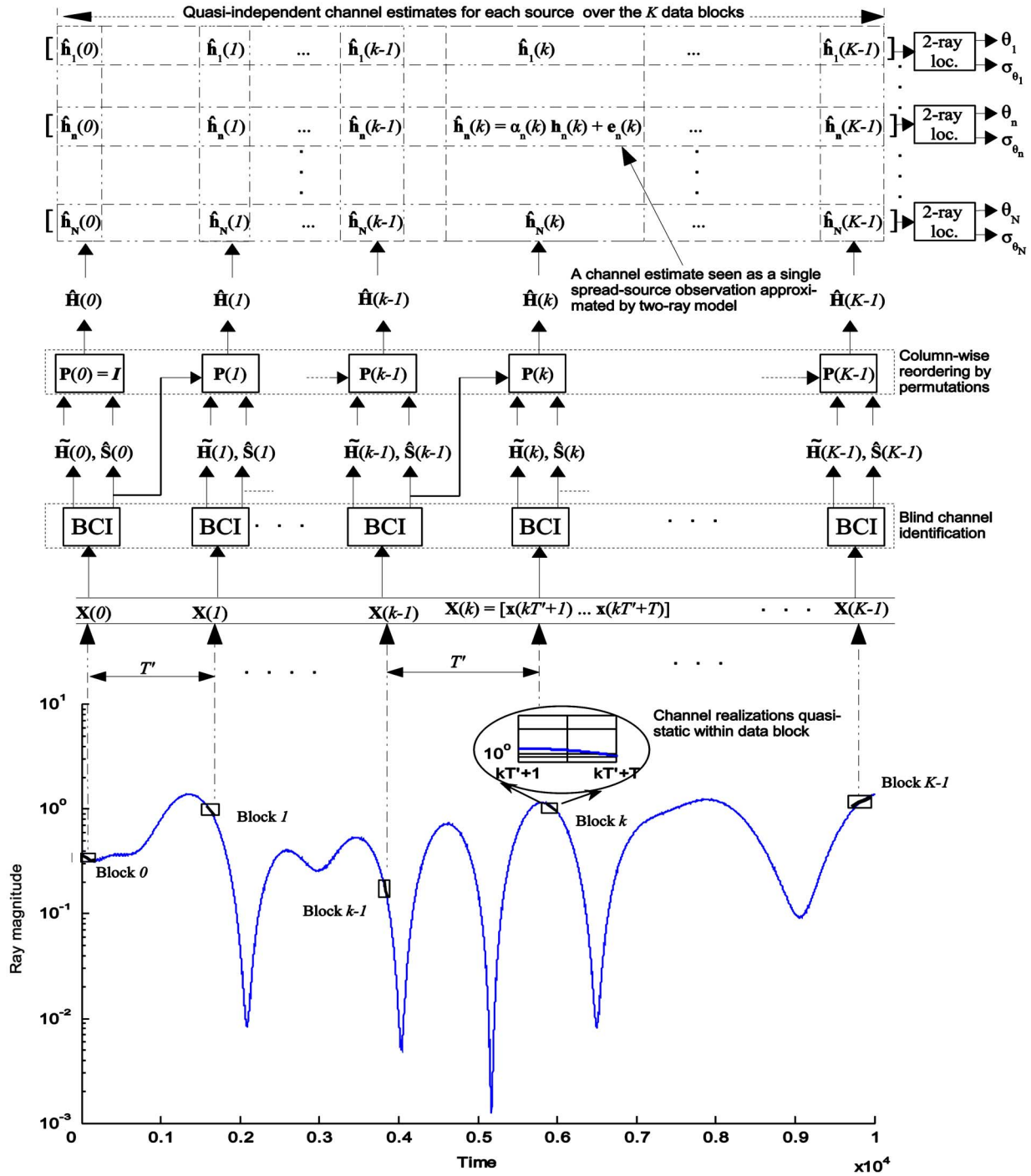


Fig. 2. An illustration of our processing strategy exploiting both fast and slow channel variations (The same processing can be performed over several interleaved sequences of enough spaced data blocks).

(they can be seen as the scattered sources in the data model considered in [1], [2], [6], and [8]). Therefore, we can successfully utilize the same two-ray approximate model proposed in [8] to estimate the AS and the nominal AoA of the n th source. Furthermore, a new technique for rays localization will be tailored. Note that this new representation is not without caveats. Indeed, the estimation error $\mathbf{e}_n(k)$ is not necessarily a spatially white process and could be correlated with $\mathbf{h}_n(k)$. Thus, one must take a special care in the channel identification stage so that this estimation error is as low as possible by a judicious

choice of a BCI algorithm that can achieve good accuracy even with few observation snapshots.¹

Finally, we consider the following covariance matrix of the n th channel vector to estimate the n th AS and nominal AoA:

$$\mathbf{R}_n = \mathbb{E}\{\mathbf{h}_n(k)\mathbf{h}_n^H(k)\} \quad (7)$$

where $(\cdot)^H$ denotes the trans-conjugate operator and $\mathbb{E}\{\cdot\}$ denotes the mathematical expectation. However, recall that only

¹Readers can refer to [26] where eight BCI algorithms are compared.

an estimate of \mathbf{h}_n is available in (6). Hence, we will approximate \mathbf{R}_n using

$$\hat{\mathbf{R}}_n = \frac{1}{K} \sum_{k=0}^{K-1} \hat{\mathbf{h}}_n(k) \hat{\mathbf{h}}_n^H(k) \quad (8)$$

which is a consistent estimator of \mathbf{R}_n up to a scale factor, $E\{|\alpha_n|^2\}$, induced by the scale indeterminacies.

B. Channel Matching

The point here is how to classify the estimated sources (or equivalently the column vectors of the random channel realizations' estimates) over the K data blocks. After running the BCI algorithm over the T samples of the k th ($k > 0$) data block, we exploit some further prior knowledge on the channel and the sources to estimate a permutation matrix $\mathbf{P}(k)$ that matches the estimated sources to those extracted from the $(k-1)$ th data block [$\mathbf{P}(0) = \mathbf{I}_N$]. The resulting estimate of the k th channel matrix realization that we will use in the sequel is then given as

$$\hat{\mathbf{H}}(k) = \tilde{\mathbf{H}}(k) \mathbf{P}^T(k). \quad (9)$$

Before going further to explain how to calculate $\mathbf{P}(k)$, we need to define a new matrix operator $\Pi\{\cdot\}$ which sets the largest entry on each row of the matrix between brackets to one and the others to zero. Then, two main scenarios can be considered.

1) *Scenario 1*: The sources are spatially very close such that the wavefronts generated from a couple of sources overlap. In this case, one has to recourse to some properties of the sources. Let $\mathbf{S}(k) \triangleq [\mathbf{s}(kT'+1) \cdots \mathbf{s}(kT'+T)]$ denote the matrix whose columns are the T samples of the source signals transmitted at the k th T -length interval, and $\hat{\mathbf{S}}(k)$ its estimate. First, suppose that the sources are correlated over time (at least between two consecutive T -length data blocks). In this case, $\mathbf{P}(k)$ can be calculated as

$$\mathbf{P}(k) = \Pi\{|\hat{\mathbf{S}}(k) \hat{\mathbf{S}}^H(k-1)|\}; \quad \forall k > 1 \quad (10)$$

where $|\cdot|$ denotes the element-wise absolute value operator. The assumption of source correlation can be further relaxed to the temporal dependence. Indeed, knowing that the sources are mutually independent, one can use some higher-order-statistics-based criteria such as maximizing the cross-cumulants [27 (pp. 19, 20)]. Other properties of the sources can also be utilized depending on the considered application. For instance, in the context of CDMA systems, one can take advantage of the spreading codes to classify the channels. For digital signals, a waveform matching of the estimated sources could be exploited if the signals have different waveforms.

2) *Scenario 2*: The sources' angular separations are much larger than the ASs such that the wavefronts generated from any couple of sources do not overlap. In contrast to *Scenario 1*, no further assumptions on the sources are required. Indeed, suppose that the permutation indeterminacy is solved over the $(k-1)$ th block, and that all the channel estimates have unit-norm columns. Then, one can calculate $\mathbf{P}(k)$ as

$$\mathbf{P}(k) = \Pi\{|\hat{\mathbf{H}}^H(k-1) \tilde{\mathbf{H}}(k)|\}. \quad (11)$$

Note that the solutions provided in *Scenario 1* apply in this case too. So far, we have investigated the BCI preprocessing step and shown how to solve the permutation indeterminacies between the consecutive K channel matrix estimates which are inherent to blind techniques. The impetus behind adding this preprocessing before attempting to recover $(\theta_n)_{1 \leq n \leq N}$ and $(\sigma_{\theta_n})_{1 \leq n \leq N}$ is, in contrast to [11] for instance, to take advantage of the inherent independence of the sources (corresponding to different users as in Fig. 1) in order to decouple the estimation of these parameters for each source apart from the others. Once these N subproblems are decoupled, the second step consists in estimating the AS and the nominal AoA of every single source. To this end, we dedicate the following section to present Taylor series expansions that have been proposed in the literature to transform the estimation of both parameters into the localization of two closely spaced, equi-powered, and uncorrelated rays [8].

IV. APPROXIMATE TWO-RAY MODEL

To have an insight into the angular spread effect on source localizers or detectors in the context of macrocell environments, a common trend has been to consider Taylor series expansions. This trend is motivated by the fact that the ASs encountered in these environments have typically small values. Specifically, a first-order Taylor series expansion has been used in [4], [5], [8] to express the spatial frequency of the n th source [see (2) and (3)] as

$$2\pi\kappa \sin(\theta_n + \tilde{\theta}_n) \approx 2\pi\kappa \sin(\theta_n) + 2\pi\kappa \tilde{\theta}_n \cos(\theta_n) \\ \triangleq \omega_n + \tilde{\omega}_n \quad (12)$$

where $\tilde{\omega}_n$ is the spatial frequency deviation resulting from the angular deviation. According to the previous representation, $\tilde{\omega}_n$ and $\tilde{\theta}_n$ have approximately the same probability density function up to a scale factor. One can also establish as in [8] that the standard deviation of $\tilde{\omega}_n$ corresponding to the n th source is expressed as:

$$\sigma_{\omega_n} = 2\pi\kappa |\cos(\theta_n)| \sigma_{\theta_n}. \quad (13)$$

Hence, determining θ_n and σ_{θ_n} amounts to estimating ω_n and $\sigma_{\omega_n} \forall n \in \{1, \dots, N\}$. Now, using this first-order Taylor series expansion, it can be established that \mathbf{R}_n is expressed as

$$\mathbf{R}_n = \mathbf{D}_a(\omega_n) \Xi(\sigma_{\omega_n}) \mathbf{D}_a^*(\omega_n) \quad (14)$$

where $(\cdot)^*$ denotes the conjugate operator

$$\mathbf{D}_a(\omega_n) = \text{diag}[\mathbf{a}(\omega_n)] \quad (15)$$

and $\Xi(\sigma_{\omega_n}) = \mathbf{R}_n$ when $\omega_n = 0$. Letting ζ_χ denote the characteristic function of a given random variable χ , the (p, r) th entry of $\Xi(\sigma_{\omega_n})$ is expressed as

$$[\Xi(\sigma_{\omega_n})]_{pr} \approx \zeta_{\tilde{\omega}_n}[(p-r)\sigma_{\omega_n}]. \quad (16)$$

This representation was exploited in [5] to explicit the effect of the angular spread on the coherence of the received signal and develop asymptotically optimal receivers. In [6], (14)–(16) have been exploited to estimate the channel parameters for the

Gaussian distribution of the angular deviation. In either case, the knowledge of the distribution of the angular deviation is crucial. To circumvent this strong assumption, a second-order Taylor series expansion of \mathbf{a} and an approximation of order $O(E\{\tilde{\omega}^4\})$ were utilized in [8] to approximate \mathbf{R}_n as

$$\mathbf{R}_n \approx \frac{1}{2} \mathbf{A}(\omega_n + \sigma_{\omega_n}, \omega_n - \sigma_{\omega_n}) \mathbf{A}^H(\omega_n + \sigma_{\omega_n}, \omega_n - \sigma_{\omega_n}) \quad (17)$$

where

$$\mathbf{A}(\omega_n + \sigma_{\omega_n}, \omega_n - \sigma_{\omega_n}) = [\mathbf{a}(\omega_n + \sigma_{\omega_n}) \mathbf{a}(\omega_n - \sigma_{\omega_n})]. \quad (18)$$

The approximation in (17)–(18) is notable. Indeed, the resulting representation is independent of the angular distribution. Rather, it explicitly depends on the nominal AoA and the AS only. More importantly, the originally complicated angular spread estimation problem is transformed into a simpler task consisting in recovering two AoAs. A point source localization algorithm could then be used to solve this problem. In [8], the focus has been on root-MUSIC [13] leading to the so-called “spread root-MUSIC.” Therein, it has been stated that the application of this localization algorithm to $\Xi(\sigma_{\omega_n})$ leads to two symmetrical values $\{\lambda(\sigma_{\omega_n}), -\lambda(\sigma_{\omega_n})\}$ where λ is a monotonous positive function which has no analytical expression, but can be empirically determined. For low σ_{ω_n} values, $\lambda(\sigma_{\omega_n}) \approx \sigma_{\omega_n}$. This approximation will be adopted in what follows.

Though it has been shown that root-MUSIC is better performing than spectral MUSIC in [17], one should note that the performance of both algorithms deteriorates as the angular separation between a couple of uncorrelated sources of interest (to localize separately) decreases especially in adverse conditions: few sensors, low SNR, and closely spaced sources. This behavior is due to the fact that the subspace decomposition is no longer easy to perform (the steering matrix is almost rank deficient and/or the noise level is high) [18]. Notice that such situations can be encountered in real-world systems where the aim is to estimate small values of the AS (or equivalently the AoAs of both closely spaced virtual rays) using few sensors due to space or cost constraints.

To sum up, the fact that the AS has typically low values in macrocell environments accounts for the Taylor series expansions that have been presented in this section to transform the estimation of the AS and the nominal AoA of a locally scattered source into the localization of two uncorrelated and equi-powered point sources. In the next section, we focus on this very particular problem (localization of two uncorrelated and equi-powered point sources) and derive new simple and accurate closed-form estimators of the AoAs of both sources. These estimators are perfectly tailored to estimate the AS and the nominal AoA of each scattered source in the data model (1).

V. LOCALIZATION OF TWO EQUI-POWERED AND UNCORRELATED POINT SOURCES

A. Model

As explained earlier, the estimation of the AS and the nominal AoA of every spread source boils down to the localization of two

closely spaced, uncorrelated and equi-powered point sources. In this section, we focus on this particular problem and propose new robust closed-form estimators for the angular separation and the mean AoA of both sources. In addition to their application here to the estimation of the AS and the nominal AoA of locally scattered sources using the approximate two-ray model, the estimators provided herein are useful in other applications where the localization of two equi-powered sources with small angular separation is of interest. To illustrate, we mention two applications: i) CDMA signature codes duplication: by implementing the proposed localization technique at the base station, the number of signature codes allocated to a single mobile terminal equipped with two closely spaced multiplexing antenna elements could be doubled (combining both spatial signatures and the allocated signature codes), and ii) satellites interference cancellation: thanks to its high accuracy, the proposed technique could be used to localize two interfering satellites with as low as 2° angular separation (e.g., geostationary satellites) and, consequently, minimize their interference.

The aforementioned applications could be modeled as follows. Suppose two source signals, $\check{\mathbf{s}}(t) = [\check{s}_1(t) \ \check{s}_2(t)]^T$, with covariance matrix $\sigma_s^2 \mathbf{I}_2$ to be localized using M sensors ($M \geq 3$). The data model is then given as in (1) but with $\mathbf{H} = \mathbf{A}(\omega_1, \omega_2)$ representing an $M \times 2$ steering matrix $[\mathbf{A}(\omega_1, \omega_2)]$ defined as in (18)² where $\omega_i = 2\pi\kappa \sin(\theta_i)$, and θ_i is the AoA of $\check{s}_i(t)$ ($i \in \{1, 2\}$)

$$\check{\mathbf{x}}(t) = \mathbf{A}(\omega_1, \omega_2) \check{\mathbf{s}}(t) + \check{\mathbf{b}}(t) \quad (19)$$

where $\check{\mathbf{b}}(t)$ represents an additive noise that we suppose independent of $\check{\mathbf{s}}(t)$. Our aim in this section is to find ω_i , $i \in \{1, 2\}$ [or equivalently θ_i , $i \in \{1, 2\}$].

B. Harmonics Estimation Using the Particular Form of the Covariance Matrix

The theoretical covariance matrix of the resulting observations is given as

$$\mathbf{R}_{\check{\mathbf{x}}} = E\{\check{\mathbf{x}}(t) \check{\mathbf{x}}^H(t)\} = \sigma_s^2 \mathbf{A}(\omega_1, \omega_2) \mathbf{A}^H(\omega_1, \omega_2) + \mathbf{\Gamma} \quad (20)$$

where $\mathbf{\Gamma}$ is the covariance matrix of the noise that we further assume here as spatially white, leading to $\mathbf{\Gamma} = \sigma^2 \mathbf{I}_M$. Notice that

$$\mathbf{R} = \mathbf{R}_{\check{\mathbf{x}}} - \sigma^2 \mathbf{I}_M = \sigma_s^2 \mathbf{A}(\omega_1, \omega_2) \mathbf{A}^H(\omega_1, \omega_2). \quad (21)$$

In practice, \mathbf{R} is unavailable, but can be estimated using a finite number T of samples as

$$\hat{\mathbf{R}} = \frac{1}{T} \sum_{t=1}^T \check{\mathbf{x}}(t) \check{\mathbf{x}}^H(t) - \hat{\sigma}^2 \mathbf{I}_M \quad (22)$$

where $\hat{\sigma}^2$ is the estimate of σ^2 obtained by averaging over the $(M - 2)$ smallest singular values of the matrix $\hat{\mathbf{R}}_{\check{\mathbf{x}}} = (1)/(T) \sum_{t=1}^T \check{\mathbf{x}}(t) \check{\mathbf{x}}^H(t)$. Our new technique localizing

²The time index k is removed because the channel is assumed to be static.

both equi-powered sources is based on the explicit expression of the entries of \mathbf{R} and the decomposition of ω_1 and ω_2 as

$$\begin{cases} \omega_1 = \omega - \delta_\omega \\ \omega_2 = \omega + \delta_\omega \end{cases} \quad (23)$$

where ω denotes the mean harmonic

$$\omega = \frac{\omega_1 + \omega_2}{2} \quad (24)$$

and $2\delta_\omega$ is the harmonics separation

$$2\delta_\omega = |\omega_1 - \omega_2|. \quad (25)$$

Consequently, finding ω_1 and ω_2 amounts to finding ω and δ_ω . Here, we mainly focus on estimating ω and δ_ω . Using (24) and (25), the entry of the m th subdiagonal of \mathbf{R} , d_m , is expressed as

$$d_m = 2\sigma_s^2 \cos(m\delta_\omega) e^{jm\omega}. \quad (26)$$

To have better estimates of $(d_m)_{0 \leq m \leq M-1}$, we exploit the Toeplitz structure of \mathbf{R} by averaging over the $M - m$ entries of the m th subdiagonals of $\hat{\mathbf{R}}$. In other words, for $m \in \{0, \dots, M - 1\}$, d_m is estimated as

$$\hat{d}_m = \frac{1}{M - m} \sum_{l=1}^{M-m} \hat{\mathbf{R}}(l + m, l). \quad (27)$$

To estimate δ_ω and ω , we use the following least square fitting (LSF) of d_m , $1 \leq m \leq M - 1$:

$$\hat{\omega}^{(m)}, \hat{\delta}_\omega^{(m)} = \arg \min_{\omega, \delta_\omega} J_m(\omega, \delta_\omega) \quad (28)$$

where

$$J_m(\omega, \delta_\omega) \triangleq |\hat{d}_m - d_m|^2. \quad (29)$$

By setting the derivatives of $J_m(\omega, \delta_\omega)$ with respect to ω and δ_ω to zero and selecting the appropriate values (minimizing J_m), the above LSF leads to the following estimators:

$$\hat{\omega}^{(m)} = \frac{1}{m} \arg(\hat{d}_m) \pm \frac{2p\pi}{m} \quad (30)$$

$$\hat{\delta}_\omega^{(m)} = \frac{1}{m} \arccos \left[\Re \left(\frac{\hat{d}_m}{\hat{d}_0} e^{-jm\omega^{(m)}} \right) \right]. \quad (31)$$

In (30) and (31), $\arg(\cdot)$ and $\Re(\cdot)$ stand for the angle and real part, respectively, $m \in \{1, \dots, M - 1\}$, $p \in \{0, \dots, \lfloor (m)/(2) \rfloor\}$, and $\lfloor \cdot \rfloor$ is the integer part operator. The superscript (m) is utilized for both estimators to specify that \hat{d}_m is utilized in (30) and (31).

Discussion:

- The estimator (31) requires a prior knowledge of the range of δ_ω . Indeed, using (31), we suppose that

$$\delta_\omega \leq \frac{\pi}{2m}. \quad (32)$$

This condition is not restrictive as one can start by using the lowest values of m (first subdiagonals of $\hat{\mathbf{R}}$) to have a

prior knowledge about the range of δ_ω , then use the first obtained results as reference values before proceeding with the largest values of m . Finally, it is important to point out that the existing localization techniques are well performing for relatively high angular separations. This fact justifies our special focus on small angular (or equivalently harmonics) separations satisfying:

$$\delta_\omega < \frac{\pi}{2(M-1)}. \quad (33)$$

- The indetermination $\pm(2p\pi)/(m)$ in (30) does not appear for $\hat{\omega}^{(1)}$. If \hat{d}_m , $m > 1$, is utilized in (30), a set of $2\lfloor (m)/(2) \rfloor + 1$ possible values can be found for $\hat{\omega}^{(m)}$. To solve this indetermination, one has to use $\hat{\omega}^{(1)}$ as a reference value and chose the optimal estimator minimizing the distance $|\hat{\omega}^{(m)} - \hat{\omega}^{(1)}|$. One might also think about combining the obtained estimates of ω and δ_ω to calculate ω_1 and ω_2 using (23) and check the orthogonality of the resulting steering vectors, $\mathbf{a}(\omega_1)$ and $\mathbf{a}(\omega_2)$, to the noise subspace (to avoid eigenvalue decompositions, one can use the analytical expression that we provide for the vector spanning the noise subspace in [28]) so as to remove the potential indeterminacies.
- The proposed solutions are perfectly tailored to estimate the AS and the nominal AoA of a scattered source. Indeed, the approximation in (17) leads to an identical form to that of \mathbf{R}_n in (21), and $\hat{\omega}^{(m)}$ in (30) [$\hat{\delta}_\omega^{(m)}$ in (31), respectively] could be successfully used to estimate ω_n (σ_{ω_n} , respectively) in (17). An important property of (30) and (31) is that they inherently reduce to the localization of a single point source when $\delta_\omega = 0$. This feature is extremely important in the localization of a single scattered source using the two-ray approximation. Indeed, if the angular spread is very small or negligible, the utilization of root-MUSIC for example to localize both rays may be misleading since the latter is unable to localize spatially very close sources with few sensors (or to appropriately localize a single source if the number of sources to be localized is erroneously set to two). To circumvent this difficulty, Bengtsson and Ottersten recurred to a ‘‘robustification’’ preprocessing to estimate the number of rays [8], thereby adding more complexity to the receiver structure.
- In terms of complexity, (30) and (31) are extremely simple to implement since no further calculations are required once the second-order statistics (SOS) are estimated to calculate ω and δ_ω . The overall complexity of the proposed two-stage approach when these closed-form estimators are used jointly with a BCI preprocessing stage is around K times the complexity of the latter since the computational cost of the former is relatively negligible. Precisely, we have a complexity of around $O[6K(1+\sqrt{N})N^2T]$ floating point operations (over KT data samples) if we use the BCI algorithm proposed in [22], [23] whose computational complexity is well established in [22].
- Some similar solutions for the mean angle of arrival only have been proposed in the literature in the case of a locally scattered source. In [9], Besson *et al.* suggested a particular form of the covariance matrix and determined the nominal

AoA using the first subdiagonal only. In [10], a Fourier transform over all the subdiagonal elements of the covariance matrix was exploited. In this paper, we suggest a general and simple approach to derive not only the nominal AoA but also the AS in the multisource case without requiring the angular distribution. In addition, we carry out in the following a theoretical investigation of the performance of the proposed estimators to deduce an optimal choice of the subdiagonal order m to estimate the required channel parameters.

C. Performance Analysis

To gain some insight into the performance of the proposed estimators (30) and (31), we investigate their asymptotic performance. To this end, we assume as in [11] that the observations in (19) are i.i.d. and circularly symmetric Gaussian. This assumption leads to the following theorem.

Theorem 1: Under the assumption of circularly symmetric Gaussian i.i.d. observations in (19), the asymptotic variances of $\hat{\omega}^{(m)}$ and $\hat{\delta}_\omega^{(m)}$ satisfy

$$\lim_{T \rightarrow +\infty} TE \left\{ \left(\hat{\omega}^{(m)} - \omega \right)^2 \right\} = \frac{\tan^2(m\delta_\omega)}{2m^2} \quad (34)$$

and

$$\lim_{T \rightarrow +\infty} TE \left\{ \left(\hat{\delta}_\omega^{(m)} - \delta_\omega \right)^2 \right\} = \frac{\frac{S(m, \delta_\omega)}{(M-m)^2} + \cos^2(m\delta_\omega)}{m^2 \sin^2(m\delta_\omega)}, \quad (35)$$

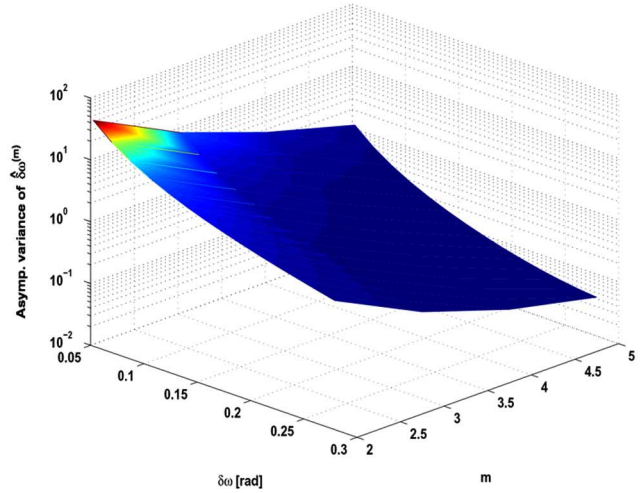
where

$$S(m, \delta_\omega) = \sum_{p,q=1}^{M-m} \cos[2(p-q)\delta_\omega]. \quad (36)$$

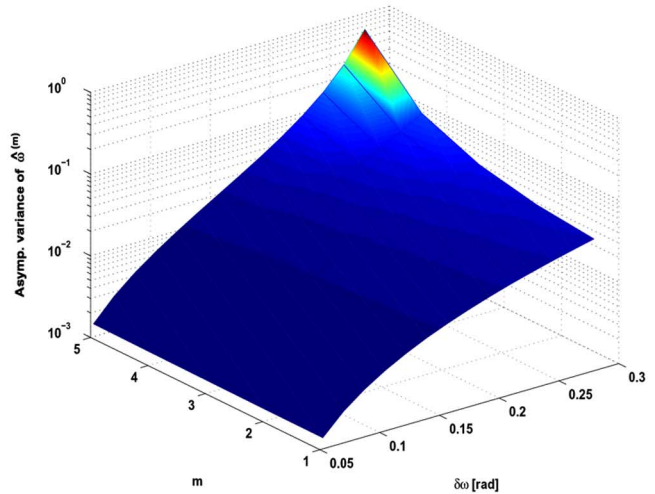
Proof: cf. Appendix I. ■

Discussion: The variations of the asymptotical variances given in (34) and (35) are depicted in Fig. 3 for the case $M = 6$. Notice that the variance of $\hat{\omega}^{(m)}$ is increasing with respect to m and δ_ω when the condition (33) is satisfied. Hence, using the first subdiagonal of the covariance matrix leads to more accurate estimates of the central harmonic. In contrast, the asymptotic variance in (34) decreases with respect to m and δ_ω . Though the above asymptotic variances have been derived under the condition of circular Gaussian and i.i.d. observations, an extensive empirical investigation showed us that these monotonous variations are also observed when the above condition on the observations is not satisfied. From this, we derive our strategy in localizing both sources. Indeed, after calculating $\hat{\mathbf{R}}$, we use its first subdiagonal to calculate the central harmonic as in (24) (i.e., for $m = 1$) and the last subdiagonal to calculate the harmonics separation as in (31) (i.e., for $m = M - 1$). Then, we estimate ω_1 and ω_2 as

$$\begin{cases} \hat{\omega}_1 = \hat{\omega}^{(1)} - \hat{\delta}_\omega^{(M-1)} \\ \hat{\omega}_2 = \hat{\omega}^{(1)} + \hat{\delta}_\omega^{(M-1)}. \end{cases} \quad (37)$$



(a)



(b)

Fig. 3. Asymptotic variances of (a) $\hat{\delta}_\omega$ and (b) $\hat{\omega}$ with respect to δ_ω and m at $M = 6$ [cf. (39) and (40)].

VI. NUMERICAL EXAMPLES

In our simulations, we will use the root mean squared error (RMSE) as a performance index as in [8]-[11]

$$\text{RMSE}(\varphi_1, \dots, \varphi_\ell) = \sqrt{\frac{1}{\ell \text{MC}} \sum_{i=1}^{\text{MC}} \sum_{l=1}^{\ell} |\varphi_l - \hat{\varphi}_l^{(i)}|^2} \quad (38)$$

where $(\varphi_l)_{1 \leq l \leq \ell}$ are the parameters to estimate, and $(\hat{\varphi}_l^{(i)})_{1 \leq l \leq \ell}$ are their estimates at the i th Monte Carlo run ($1 \leq i \leq \text{MC}$). In all of the investigated scenarios, we take $\text{MC} = 10^3$. To have a better insight into the results, the RMSE and the Cramèr-Rao lower bound (CRLB) values will be presented in degrees.

A. Localization of Two Uncorrelated Point Sources

As it has been stated in Section V, the proposed two-ray localization approach, in addition of being tailored to the estimation of the AS and the nominal AoA of a locally scattered source

(cf. Section IV), applies to multiple situations when the localization of two equi-powered and spatially close point sources is of interest. Therefore, we dedicate this subsection to empirically investigate its performance. To that end, we compare it to root-MUSIC and one of its recently proposed variations (root-MUSIC-like) for non circular and uncorrelated sources [32]. The efficiency of the latter has been demonstrated in [33]. We also plot the square-root of the CRLB.³ For fair comparisons, we chose the scenario of two BPSK sources (noncircular sources so that the root-MUSIC-like algorithm can be applied though our approach does not require this assumption) propagating along two closely spaced plane waves (i.e., no scattering). We run the algorithms over one data block (i.e., $K = 1$) of length $T = 200$. We aim at localizing two sources located at θ_1 and θ_2 [without loss of generality (w.l.o.g.), $\theta_1 \leq \theta_2$] using a ULA of three or six sensors depending on the investigated scenario.

In Figs. 4 and 5, we plot $\text{RMSE}(\theta_1, \theta_2)$ with respect to the angular separation $\Delta\theta = \theta_2 - \theta_1$ (at SNR = 10 dB) and the SNR (at $\Delta\theta = 3^\circ$), respectively, for three and six sensors. In both figures, we notice that root-MUSIC's accuracy deteriorates when the signals are closely spaced or the SNR decreases. This fact is due to its inherent behavior in the case of an almost rank-deficient steering matrix investigated in some earlier works [17], [18]. The root-MUSIC-like algorithm takes advantage of the noncircularity of the sources to provide more accurate results than the latter but its performance is still remarkably affected when the SNR or the angular separation decreases. In contrast, the proposed approach exhibits a regular behavior and achieves good accuracy and high SNR gains even with three sensors only. The fact that the closed-form estimators (37) were developed under very particular hypotheses on the two point sources (equi-powered, uncorrelated, and closely spaced) following a covariance matching reasoning (which is known to be an alternative to ML [34]) accounts for their superiority when compared to other localization techniques which are quite general and do not exploit all these properties. Therefore, one can conclude that these estimators may be of great interest for applications where the localization of two closely spaced point sources in adverse situations (few sensors and low SNR) is of interest. Notice also that $\text{RMSE}(\theta_1, \theta_2)$ achieved by the new method is lower bounded when the SNR is high. This lower bound is set by the inaccuracy in estimating the SOS as it has been shown in Section V-C. However, one should note that this is not actually a serious limitation since this lower bound is acceptable ($\approx 0.1^\circ$) and appears only for very high SNR values rarely encountered in practical real-world applications.

B. Channel Parameters Estimation in the Case of Locally Scattered Sources

Here, we start by demonstrating the advantages of the application of the proposed two-point source localization technique to the estimation of the AS and the nominal AoA of a

³The CRLB for AoA estimation has been determined for some particular cases: deterministic or conditional data model [18], Gaussian sources [29], and some random discrete signals mainly BPSK and QPSK [30]. The derivation of this lower bound is beyond the scope of this paper. Since we consider BPSK sources, we use the CRLB provided in [30].

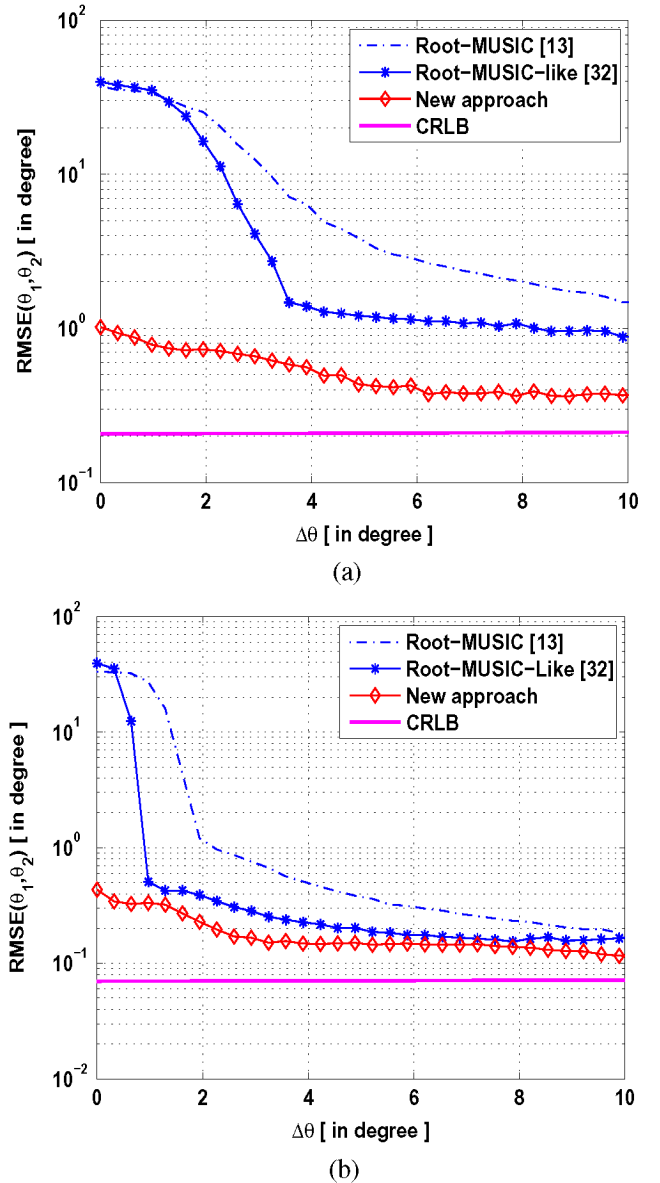


Fig. 4. Case of two point sources— $\text{RMSE}(\theta_1, \theta_2)$ versus $\Delta\theta$ at SNR = 10 dB using: (a) three sensors, (b) six sensors.

single locally spread source (justified by the two-ray approximate model). Afterwards, we prove the efficiency of the proposed two-stage algorithm in decoupling and accurately estimating the channel spatial parameters in presence of multiple locally spread sources. To model the local scattering, we will set the number of the incoming wavefronts from every source to $L = 50$ in all the simulations as in [8]. Notice that L has typically large values in radio communication environments [3], [34]. We will further assume, w.l.o.g., that the angular deviations $(\hat{\theta}_n)_{1 \leq n \leq N}$ in the data model (1)–(2) are Gaussian distributed (some results for uniform distribution can be found in [31]).

1) *Case of a Single Locally Scattered Source:* We implement the data model in (1) for a BPSK source located at $\theta = 10^\circ$ with an AS $\sigma_\theta = 3^\circ$. To satisfy the incoherent distribution of the source with the Rayleigh fading model in (1)–(2) with a

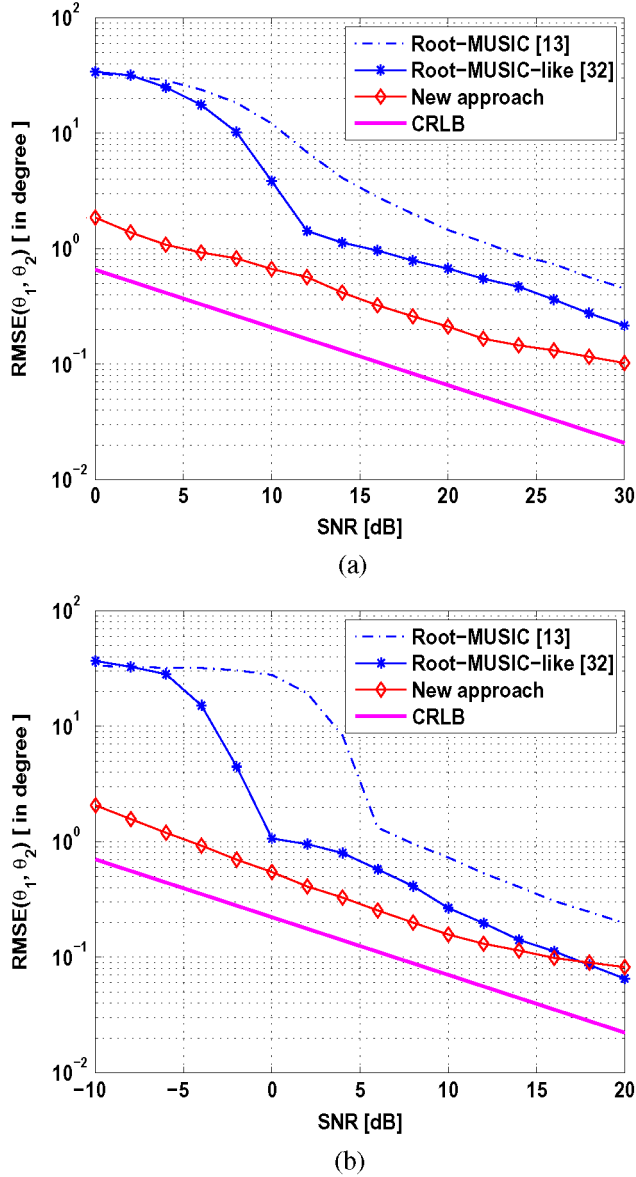


Fig. 5. Case of two point sources—RMSE(θ_1, θ_2) versus SNR at $\Delta\theta = 3^\circ$ using: (a) three sensors, (b) six sensors.

single source ($N = 1$), we consider L Gaussian and i.i.d. coefficients $(\gamma_l)_{1 \leq l \leq L}$ (the subscript $n = 1$ is removed for the sake of clarity) which vary independently from one snapshot to another (by spacing samples) as it is commonly assumed in the literature (e.g., [6], [8]) and we estimate the SOS using $T_w = 200$ observation snapshots. In other words, we have $K = 200$, $T = 1$, and $T' = 0$. Figs. 6 and 7 present the performance of the provided technique compared to spread root-MUSIC [8], the iterative algorithm in [11] which is to our knowledge a method of choice as it achieves high accuracy without the knowledge of the angular distribution, and the theoretical CRLB⁴ using three and six sensors.

⁴The CRLB can be derived in the case of a single source when it satisfies two key properties: i) the source's temporal realizations are i.i.d.; ii) the source's magnitude $|s(t)|^2$ is constant. Then, the Fisher Information matrix can be derived and the CRLB can be numerically calculated [35].

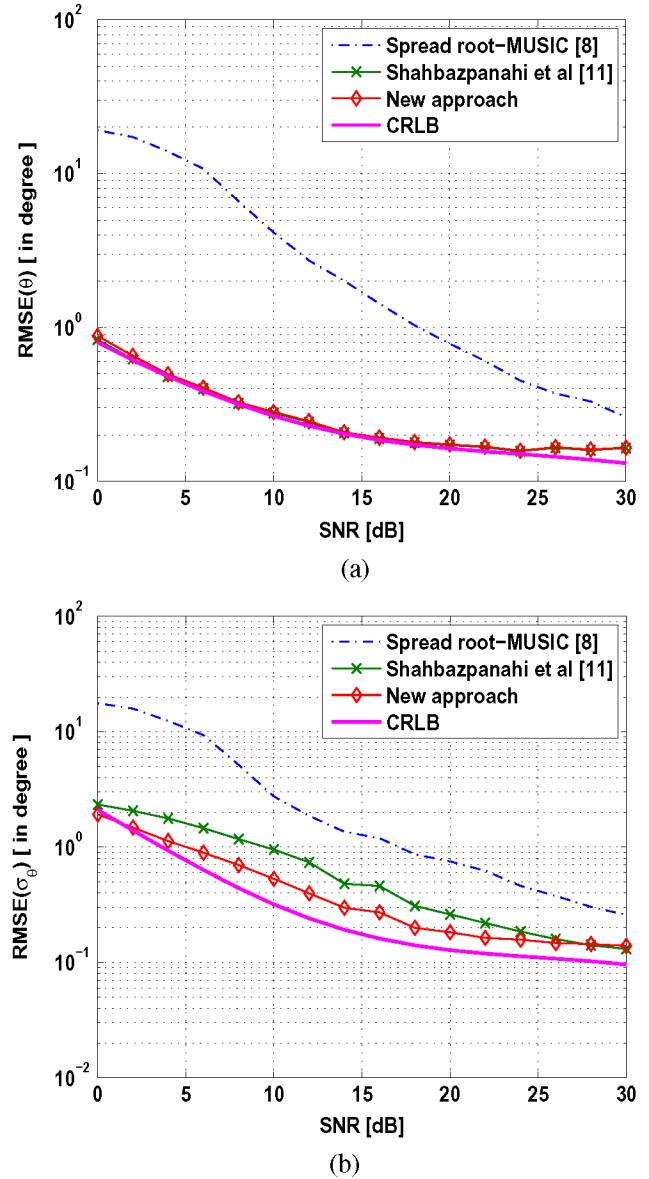


Fig. 6. Case of a single scattered source—Performance with respect to SNR at $\sigma_\theta = 3^\circ$ using three sensors: (a) RMSE(θ). (b) RMSE(σ_θ).

The estimators provided in Section V are closed-form and require very low computational cost once the observations covariance matrix is calculated. Hence, one can use any of the $(M-1)$ subdiagonals to estimate the nominal AoA and the AS. To obtain a better estimate of θ , one has to resort to the first subdiagonals. Regarding the AS estimate, it is recommended to resort to the last subdiagonals provided that the AS satisfies the condition in (32). In Fig. 6, we found that the second subdiagonal ($m = 2$) of the observations' covariance matrix gives the best accuracy to the estimation of both parameters. In Fig. 7, we use the second subdiagonal ($m = 2$) to estimate θ and the 4th subdiagonal ($m = 4$) to estimate σ_θ . In either case, we notice that the new two-point source localization technique dramatically improves the accuracy of the required parameters. The resulting RMSE(θ) and RMSE(σ_θ) are almost optimal (overlap with the

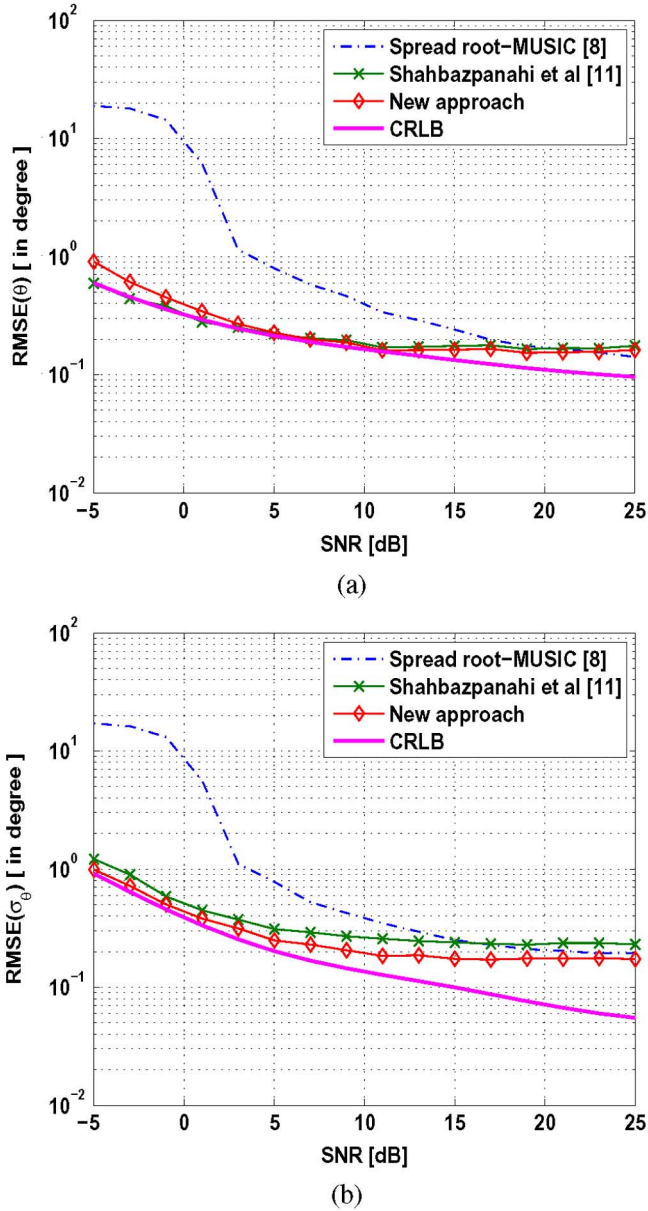


Fig. 7. Case of a single scattered source—Performance with respect to SNR at $\sigma_\theta = 3^\circ$ using six sensors: (a) $\text{RMSE}(\theta)$. (b) $\text{RMSE}(\sigma_\theta)$.

CRLB) when the SNR has low to moderate values. The algorithm [11] is also highly performing, especially for source localization, but it fails to achieve a better estimate of the AS than the proposed closed-form estimators. More importantly, the algorithm proposed in [11] is iterative and requires a prior estimate of the source location (for initialization), thereby adding more complexity to the design of the receiver. In contrast, one can obviously notice that the implementation of the provided method is straightforward as neither iterations nor initializations are involved. As the SNR increases, the accuracy of the three techniques saturates. This lower bound is mainly⁵ due to the approximations presented in Section IV and those utilized by Shahbazpanahi *et al.* in [11].

⁵The effect of the SOS estimation inaccuracy observed in Fig. 5 is negligible since all algorithms almost have the same lower bound for high SNR values.

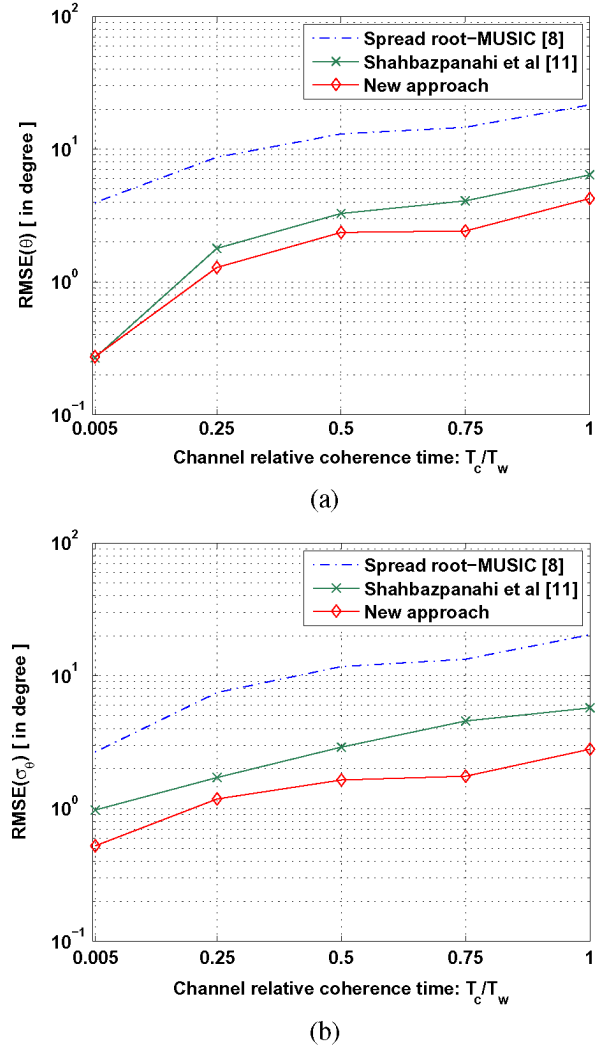


Fig. 8. Effect of the channel quasi-static behavior on the accuracy of the two-ray approximation using three sensors at $\sigma_\theta = 3^\circ$, and SNR = 10 dB. (a) $\text{RMSE}(\theta)$. (b) $\text{RMSE}(\sigma_\theta)$, $T_w = 2 \cdot 10^2$.

Now, we investigate the effect of the channel coherence time on the performance of the AS and nominal AoA estimation. We consider the same case of a BPSK source located at $\theta = 10^\circ$ and having $\sigma_\theta = 3^\circ$ as AS. To simulate the quasi-static variations of the channel, we suppose that it is invariant over a T_c duration length that we increase gradually. Letting $T_w = 200$ denote the overall observation window (with $T_c \leq T_w$), T_c/T_w is the relative coherence time (the inverse of K which is the number of independent channel realizations during T_w snapshots in this case). Such situation is typically encountered in a burst-mode operating system (cf. [1] and references therein). Fig. 8 shows how the channel parameters estimation accuracy deteriorates as the channel relative coherence time increases. To overcome this performance deterioration, larger sampling periods (exceeding the coherence time) and observation windows must be considered. In the following, we show the gain achieved by our new two-stage approach to estimate the channel parameters in the case of multiple spread sources.

TABLE I
TWO-STAGE ALGORITHM TO ESTIMATE THE NOMINAL AOAS AND THE ASS OF LOCALLY SCATTERED SOURCES

1. Initialization
Knowing T_c , chose T , T' , and K such that:
(i) Condition (4) is satisfied with T sufficiently large to enable blind channel identification.
(ii) K large enough to have good estimates of channel parameters.
2. For $k = 0 : K - 1$
(i) BCI over the k th data block $\mathbf{X}(k) = [\mathbf{x}(kT' + 1) \dots \mathbf{x}(kT' + T)]$ (e.g., using [22], [23]):
$\tilde{\mathbf{H}}(k) = \text{BCI}[\mathbf{X}(k)]$.
(ii) Estimate the sources (using the MMSE criterion):
$\hat{\mathbf{S}}(k) = \tilde{\mathbf{H}}^H(k) [\mathbf{X}(k)\mathbf{X}^H(k)/T]^{-1} \mathbf{X}(k)$.
(iii) Match the channels depending on the scenario [cf. Subsection III-B. In Scenario 2, source estimation is optional]:
$\hat{\mathbf{H}}(k) = \tilde{\mathbf{H}}(k)\mathbf{P}^T(k)$.
End For
3. For $n = 1 : N$
(i) Calculate the covariance matrix given by (8).
(ii) Estimate ω_n as in (30).
(iii) Deduce θ_n as: $\theta_n = \arcsin\left(\frac{\omega_n}{2\kappa\pi}\right)$.
(iv) Estimate σ_{ω_n} as in (31).
(v) Deduce σ_{θ_n} as: $\sigma_{\theta_n} = \frac{\sigma_{\omega_n}}{2\kappa\pi \cos(\theta_n)}$.
End For

2) *Case of Multiple Locally scattered Sources:* Here, we implement our two-stage algorithm given in Table I. As described above, we start by blindly estimating the channel by means of the algorithm proposed in [22], [23] (this choice is not restrictive and is motivated by the suitability of this algorithm to the investigated scenario in terms of accuracy and complexity; refer to [22], [23], and [26] for further details). Then, we match the channel components to estimate the required parameters for each source using the two-ray approximation followed by the two-point source localization algorithm. We consider two BPSK sources located at $\theta_1 = 5^\circ$ and θ_2 that will be chosen depending on the investigated situation. The ASs of both sources are chosen as $\sigma_{\theta_1} = \sigma_{\theta_2} = 3^\circ$, w.l.o.g. In order to match the channel components, one must resort to the solutions provided in Section III-B. Here, we suppose that the same signals are retransmitted during all the K intervals. The variables γ_n and $\tilde{\theta}_n$, $n \in \{1, 2\}$, characterizing the channel are assumed to be constant over every T -length data block but varying from one interval to another following a Gaussian distribution. We chose $T = K = 200$ so that we ensure an acceptable accuracy in blindly estimating the channel matrix realizations, the ASs, and the nominal AoAs while keeping reasonable complexity.⁶ We compare the proposed approach using root-MUSIC and the new two-point source localization technique to the direct one where we calculate the SOS over the KT snapshots and use root-MUSIC to localize twice the number of sources as described in [8]. For the latter technique, the virtual rays are paired together two by two. Then, each source's AS and nominal AoA are estimated using these pairs. Notice here that a major limitation of the latter arises. Indeed, the required number of sensors must satisfy $M > 2N$ as a subspace method is utilized to localize the rays. In contrast, the two-stage approach requires only

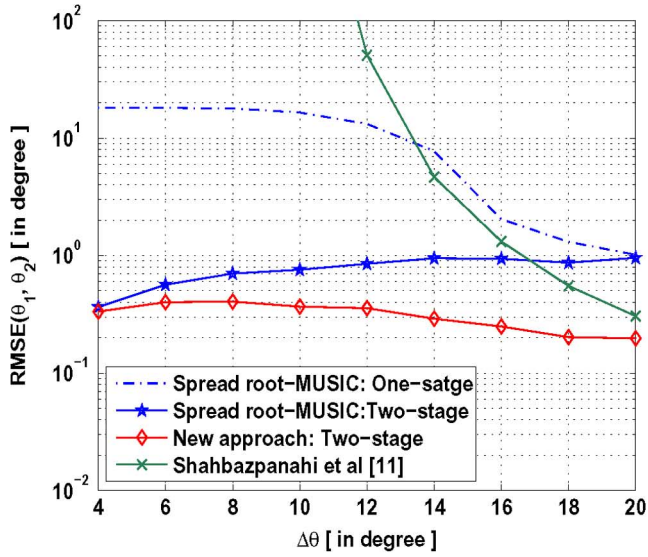
⁶Simulations, not shown for lack of space, suggest that the RMSE of channel parameters decreases versus K and T and reaches acceptable levels for $K = T = 200$.

$M = 3$ sensors to localize the two rays for every source and $M \geq N$ for the channel identification preprocessing. For fair comparisons, we chose $M = 6$. In what follows, we investigate the performance of the two-stage technique to the angular separation between the sources and the SNR. Since [11] is among the few methods that have been recently proposed to estimate the ASs and the nominal AoAs of multiple spread sources, we include it in our comparisons.

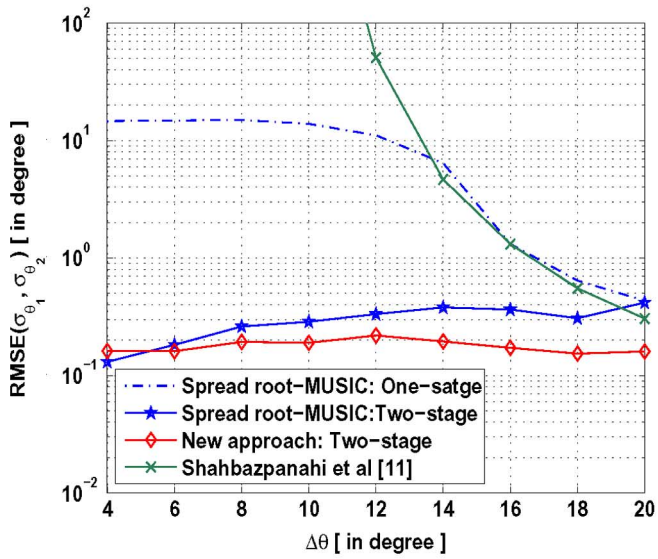
Now, we fix the SNR at 5 dB⁷ and vary the AoA of the second source. Fig. 9 shows the achieved $\text{RMSE}(\theta_1, \theta_2)$ and $\text{RMSE}(\sigma_{\theta_1}, \sigma_{\theta_2})$ values with respect to $\Delta\theta = \theta_2 - \theta_1$. For very close sources whose wavefronts overlap⁸ [i.e., $(\sigma_{\omega_1} + \sigma_{\omega_2}) > (\omega_2 - \omega_1)$], virtual rays pairing is misleading (we assume w.l.o.g that $\omega_2 \geq \omega_1$). Even when the wavefronts do not overlap (e.g., $\Delta\theta > 6^\circ$), the virtual steering matrix $\mathbf{A}(\omega_1 - \sigma_{\omega_1}, \omega_1 + \sigma_{\omega_1}, \omega_2 - \sigma_{\omega_2}, \omega_2 + \sigma_{\omega_2})$ might be almost rank deficient when $(\omega_1 + \sigma_{\omega_1})$ and $(\omega_2 - \sigma_{\omega_2})$ are very close. This fact has a detrimental effect on parameters estimation using the one-stage spread root-MUSIC since the sources are not processed separately. Similarly, the algorithm proposed in [11] is severely affected for low angular separations (we even found that for $\Delta\theta < 10^\circ$ this algorithm fails from its first iteration though it had been initialized at $\theta_1 + 2^\circ$ and $\theta_2 + 2^\circ$; more details can be found in [11]). By further taking into account the sources' independence, the proposed two-stage processing is able to identify the corresponding channels separately and accurately determine their parameters especially when the new proposed two-point-source localization technique is utilized in the second stage. In the second scenario, we chose $\theta_2 = 15^\circ$ and assess the effect of the SNR on $\text{RMSE}(\theta_1, \theta_2)$ and $\text{RMSE}(\sigma_{\theta_1}, \sigma_{\theta_2})$. The results are presented in Fig. 10. The algorithm of [11] is discarded from our comparisons because

⁷We suppose, w.l.o.g., that both sources are of unit power and we use this definition: $\text{SNR} = 10 \log_{10}(1/\sigma_b^2)$.

⁸For $\Delta\theta = 4^\circ$, we have $\sigma_{\omega_1} + \sigma_{\omega_2} \approx 18.7^\circ$ and $\omega_2 - \omega_1 \approx 12.5^\circ$.



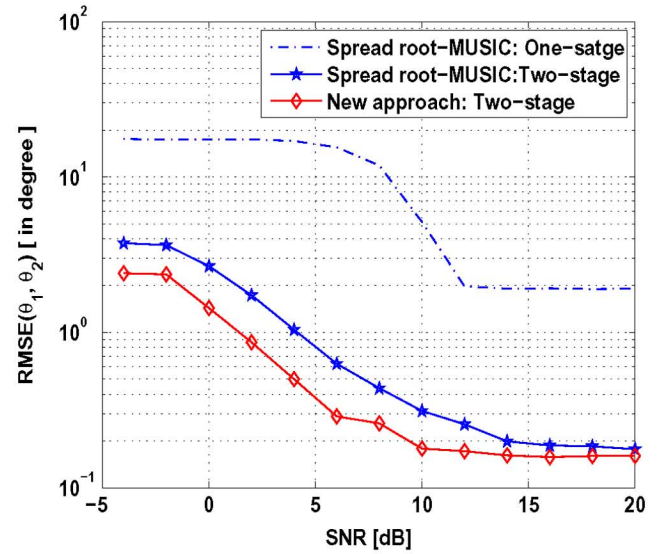
(a)



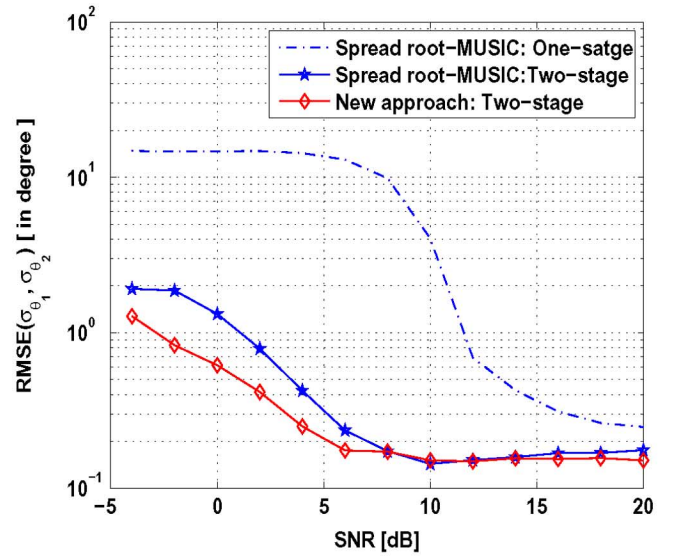
(b)

Fig. 9. Case of two scattered sources—Performance with respect to angular separation between both sources using six sensors at $\sigma_{\theta_1} = \sigma_{\theta_2} = 3^\circ$, SNR = 5 dB, and $\theta_1 = 5^\circ$: (a) $\text{RMSE}(\theta_1, \theta_2)$. (b) $\text{RMSE}(\sigma_{\theta_1}, \sigma_{\theta_2})$.

it fails to converge for the corresponding angular separation as illustrated in Fig. 9. Notice how the two-stage procedure leads to tremendous SNR gains compared to the one-stage. In addition, the new two-point localization technique achieves more accurate results in the case of very low SNR values. Finally, it is worth mentioning that the new idea of decoupling the multisource estimation problem into independent single-source channel estimation problems can be utilized jointly with other algorithms for channel spatial parameters estimation in the second stage as the one proposed in [11]. This would lead to comparable if not poorer results especially for source location as it can be inferred from Figs. 6 and 7, yet at some additional computational and implementation complexity at the second stage when compared to the proposed direct closed-form estimators as neither iterations nor initializations are required by the latter.



(a)



(b)

Fig. 10. Case of two scattered sources—Performance with respect to SNR using six sensors at $\sigma_{\theta_1} = \sigma_{\theta_2} = 3^\circ$, $\theta_1 = 5^\circ$, and $\theta_2 = 15^\circ$. (a) $\text{RMSE}(\theta_1, \theta_2)$. (b) $\text{RMSE}(\sigma_{\theta_1}, \sigma_{\theta_2})$.

VII. CONCLUSION

In this paper, we proposed a two-stage approach for channel parameters (angular spreads and nominal angles of arrival) estimation using a uniform linear array of sensors for locally scattered sources. We exploited both short- and long-term typical variations of the wireless channel. First, we took advantage of the channel's quasi-static behavior over short periods of time to blindly estimate it over several data blocks regularly spaced by intervals larger than the coherence time in order to decouple the multisource channel parameters estimation problem in hand into independent and parallel single-source channel parameters estimation subproblems. Second, for each spatially scattered source, we separately processed the corresponding sequence of the channel realization estimates as a new single-scattered-

source observation over which we applied Taylor series expansions to transform the estimation of its nominal angle of arrival and angular spread into a simple localization of two closely spaced, equi-powered, and uncorrelated point sources. Then, we proposed new closed-form estimators for the mean value and the separation of the spatial harmonics of both rays. We proved through some analytical and empirical investigations that these closed-form estimators are efficient. Finally, we applied the new localization algorithm to retrieve the angular spread and the nominal angle of arrival of every scattered source. Simulation results revealed that the proposed two-stage strategy is able to achieve high precision by separately estimating the required parameters even for arrays of moderate size, at relatively low SNR values, and in worst-case scattering scenarios.

APPENDIX I PROOF OF THEOREM 1

We derive these results by proceeding as in [10] where the focus has been on the localization of a locally scattered source. Let $\xi_m = |d_m| = d_0 \cos(m\delta_\omega)$. Then, following [10], we can prove that:

$$\lim_{T \rightarrow +\infty} TE \left\{ \left(\hat{\omega}^{(m)} - \omega \right)^2 \right\} = \frac{\lim_{T \rightarrow +\infty} TE \left\{ \left(\frac{\partial J_m}{\partial \omega} \right)^2 \right\}}{\left[\lim_{T \rightarrow +\infty} \frac{\partial^2 J_m}{\partial \omega^2} \right]^2} \quad (39)$$

$$\text{and} \quad \lim_{T \rightarrow +\infty} TE \left\{ \left(\hat{\delta}_\omega^{(m)} - \delta_\omega \right)^2 \right\} = \frac{\lim_{T \rightarrow +\infty} TE \left\{ \left(\frac{\partial J_m}{\partial \delta_\omega} \right)^2 \right\}}{\left[\lim_{T \rightarrow +\infty} \frac{\partial^2 J_m}{\partial \delta_\omega^2} \right]^2}. \quad (40)$$

These derivatives are evaluated at the actual parameters. Next, it can be shown using (29) that

$$\begin{aligned} \frac{\partial J_m}{\partial \omega} &= -2m\xi_m \Im \{ \hat{d}_m e^{-jm\omega} \} \\ \frac{\partial^2 J_m}{\partial \omega^2} &= 2m^2 \xi_m \Re \{ \hat{d}_m e^{-jm\omega} \} \\ \frac{\partial J_m}{\partial \delta_\omega} &= -2md_0 \sin(m\delta_\omega) [\xi_m - \Re(\hat{d}_m e^{-jm\omega})] \\ \frac{\partial^2 J_m}{\partial \delta_\omega^2} &= 2m^2 d_0^2 \sin^2(m\delta_\omega) - 2m^2 \xi_m [\xi_m - \Re(\hat{d}_m e^{-jm\omega})]. \end{aligned}$$

Using the i.i.d. property of the observations, it can be shown that

$$\lim_{T \rightarrow +\infty} \frac{\partial^2 J_m}{\partial \omega^2} = 2m^2 \xi_m^2 \quad (41)$$

$$\lim_{T \rightarrow +\infty} \frac{\partial^2 J_m}{\partial \delta_\omega^2} = 2m^2 d_0^2 \sin^2(m\delta_\omega). \quad (42)$$

To calculate the numerators in (39) and (40), we use the circular Gaussian and i.i.d. property of the observations jointly with the

fact that for a given complex variable χ , $\Re^2(\chi) = 1/2[|\chi|^2 + \Re(\chi^2)]$ and $\Im^2(\chi) = (1/2)[|\chi|^2 - \Re(\chi^2)]$ where $\Im(\cdot)$ denotes the imaginary part. Hence, we have

$$\begin{aligned} E \left\{ \left(\frac{\partial J_m}{\partial \omega} \right)^2 \right\} &= 4m^2 \xi_m^2 E \left\{ \Im^2 \left(\hat{d}_m e^{-jm\omega} \right) \right\} \\ &= 2m^2 \xi_m^2 E \left\{ |\hat{d}_m|^2 - \Re \left(\hat{d}_m^2 e^{-2jm\omega} \right) \right\} \quad (43) \end{aligned}$$

and

$$\begin{aligned} E \left\{ \left(\frac{\partial J_m}{\partial \delta_\omega} \right)^2 \right\} &= 4m^2 d_0^2 \sin^2(m\delta_\omega) \\ &\quad \times \left[\xi_m^2 + E \left\{ \Re^2 \left(\hat{d}_m e^{-jm\omega} \right) \right\} \right. \\ &\quad \left. - 2\xi_m E \left\{ \Re \left(\hat{d}_m e^{-jm\omega} \right) \right\} \right] \\ &= 4m^2 d_0^2 \sin^2(m\delta_\omega) \\ &\quad \times \left[-\xi_m^2 + E \left\{ \Re^2 \left(\hat{d}_m e^{-jm\omega} \right) \right\} \right] \\ &= 4m^2 d_0^2 \sin^2(m\delta_\omega) \left[-\xi_m^2 \right. \\ &\quad \left. + \frac{1}{2} E \left\{ |\hat{d}_m|^2 + \Re \left(\hat{d}_m^2 e^{-2jm\omega} \right) \right\} \right]. \quad (44) \end{aligned}$$

Here, we exploit the following result provided in [9], [10] for circular Gaussian and i.i.d. observations:

$$\begin{aligned} E \left\{ |\hat{d}_m|^2 \right\} &= |d_m|^2 + \frac{1}{T(M-m)^2} \\ &\quad \times \sum_{p=1}^{M-m} \sum_{q=1}^{M-m} \mathbf{R}(p+m, q+m) \mathbf{R}(q, p) \quad (45) \end{aligned}$$

and

$$\begin{aligned} E \left\{ \hat{d}_m^2 \right\} &= d_m^2 + \frac{1}{T(M-m)^2} \sum_{p=1}^{M-m} \\ &\quad \times \sum_{q=1}^{M-m} \mathbf{R}(p+m, q) \mathbf{R}(q+m, p). \quad (46) \end{aligned}$$

Taking into account the explicit expressions of the entries of \mathbf{R} in (45) and (46), we find that

$$\begin{aligned} E \{ |\hat{d}_m|^2 \} &= \xi_m^2 + \frac{d_0^2}{2T(M-m)^2} [S(m, \delta_\omega) + (M-m)^2] \quad (47) \end{aligned}$$

and

$$\begin{aligned} E \left\{ \hat{d}_m^2 \right\} e^{-2jm\omega} &= \xi_m^2 + \frac{d_0^2}{2T(M-m)^2} \\ &\quad \times [S(m, \delta_\omega) + (M-m)^2 \cos(2m\delta_\omega)] \quad (48) \end{aligned}$$

where $S(m, \delta_\omega)$ is as defined in (36). Injecting (47) and (48) in (43) and (44), we obtain

$$\begin{aligned} E \left\{ \left(\frac{\partial J_m}{\partial \omega} \right)^2 \right\} \\ = \frac{4m^2 d_0^4 \sin^2(m\delta_\omega)}{T} \left[\frac{S(m, \delta_\omega)}{(M-m)^2} + \cos(m\delta_\omega) \right] \end{aligned} \quad (49)$$

and

$$\begin{aligned} E \left\{ \left(\frac{\partial J_m}{\partial \delta_\omega} \right)^2 \right\} \\ = \frac{2m^2 \xi_m^2 \sin^2(m\delta_\omega)}{T}. \end{aligned} \quad (50)$$

Using (41), (42), (49), and (50) jointly with (39) and (40), we directly obtain (34) and (35). ■

ACKNOWLEDGMENT

The authors would like to thank the anonymous reviewers for their valuable comments and suggestions.

REFERENCES

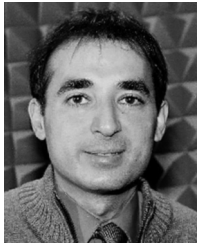
- [1] D. Astély and B. Ottersten, "The effects of local scattering on direction of arrival estimation with MUSIC," *IEEE Trans. Signal Process.*, vol. 47, no. 12, pp. 3220–3234, Dec. 1999.
- [2] B. Ottersten, "Array processing for wireless communications," in *Proc. 8th IEEE Signal Process. Workshop Statist. Signal Array Process.*, 1996, pp. 466–473.
- [3] P. Zetterberg and B. Ottersten, "The spectrum efficiency of a base-station antenna array system for spatially selective transmission," *Proc. IEEE 43rd VTC*, pp. 7–15, 1994.
- [4] S. Kikuchi, A. Sano, H. Tisujji, and R. Miura, "Mobile localization using local scattering model in multipath environments," *Proc. IEEE 60th VTC*, pp. 339–343, 2004.
- [5] A. M. Rao and D. L. Jones, "Efficient detection with arrays in the presence of angular spreading," *IEEE Trans. Signal Process.*, vol. 51, no. 2, pp. 301–312, Feb. 2003.
- [6] T. Trump and B. Ottersten, "Estimation of nominal direction of arrival and angular spread using an array of sensors," *Signal Process.*, vol. 50, no. 1–2, pp. 57–69, Apr. 1996.
- [7] Y. Meng, P. Stoica, and K. Wong, "Estimation of the directions of arrival of spatially dispersed signals in array processing," *Inst. Elect. Eng. Proc. Radar, Sonar, Navigat.*, vol. 143, pp. 1–9, Feb. 1996.
- [8] M. Bengtsson and B. Ottersten, "Low-complexity estimators for distributed sources," *IEEE Trans. Signal Process.*, vol. 48, no. 8, pp. 2185–2194, Aug. 2000.
- [9] O. Besson, F. Vincent, P. Stoica, and A. Gershman, "Approximate maximum likelihood estimators for array processing in multiplicative noise environments," *IEEE Trans. Signal Process.*, vol. 48, no. 9, pp. 2185–2194, Sep. 2000.
- [10] O. Besson, P. Stoica, and A. B. Gershman, "Simple and accurate direction of arrival estimator in the case of imperfect spatial coherence," *IEEE Trans. Signal Process.*, vol. 49, no. 4, pp. 730–737, Apr. 2001.
- [11] S. Shahbazpanahi, S. Valaee, and A. B. Gershman, "A covariance fitting approach to parametric localization of multiple incoherently distributed sources," *IEEE Trans. Signal Process.*, vol. 52, no. 3, pp. 592–600, Mar. 2004.
- [12] R. Ertel, P. Cardieri, K. Sowerby, T. S. Rappaport, and J. Reed, "Overview of the spatial channel models for antenna array communication systems," *IEEE Pers. Commun.*, vol. 5, no. 1, pp. 10–22, Feb. 1998.
- [13] A. J. Barabell, "Improving the resolution of eigenstructure-based direction finding algorithms," *Proc. IEEE ICASSP*, pp. 336–339, 1983.
- [14] P. Stoica and K. C. Sharman, "Novel eigenanalysis method for direction estimation," *IEE Proc. F Radar, Signal Process.*, vol. 137, no. 1, pp. 19–26, Feb. 1990.
- [15] R. Roy and T. Kailath, "ESPRIT-estimation of signal parameters via rotational invariance techniques," *IEEE Trans. Acoust., Speech, Signal Process.*, vol. 37, no. 7, pp. 984–995, Jul. 1989.
- [16] R. O. Schmidt, "Multiple emitter location and signal parameter estimation," *IEEE Trans. Antennas Propag.*, vol. 34, no. 3, pp. 276–280, Mar. 1986.
- [17] B. D. Rao and K. V. S. Hari, "Performance analysis of root-MUSIC," *IEEE Trans. Acoust., Speech, Signal Process.*, vol. 37, no. 12, pp. 1939–1949, Dec. 1989.
- [18] P. Stoica and A. Nehorai, "MUSIC, maximum likelihood, and Cramer-Rao bound," *IEEE Trans. Acoust., Speech, Signal Process.*, vol. 38, no. 12, pp. 720–741, May 1989.
- [19] H. Arslan and G. E. Bottomley, "Channel estimation in narrowband wireless communication systems," *Wireless Commun. Mob. Comput.*, vol. 1, no. 1, pp. 201–219, Mar. 2001.
- [20] L. Albera, A. Ferréol, P. Chevalier, and P. Comon, "ICAR: a tool for blind source separation using fourth order statistics only," *IEEE Trans. Signal Process.*, vol. 53, no. 10, pp. 3633–3643, Oct. 2005.
- [21] L. Tong, R. Liu, and Y. H. V. Soon, "Indeterminacy and identifiability of blind identification," *IEEE Trans. Circuits Syst.*, vol. 38, no. 5, pp. 499–509, May 1991.
- [22] P. Comon, "Independent component analysis, a new concept?," *Signal Process.*, vol. 36, no. 3, pp. 287–314, Apr. 1994.
- [23] P. Comon and E. Moreau, "Improved contrast dedicated to blind separation in communications," *Proc. IEEE ICASSP*, vol. 5, pp. 3453–3456, 1997.
- [24] J.-F. Cardoso and A. Souloumiac, "Blind beamforming for non-Gaussian signals," *Inst. Elect. Eng. Proc. Radar, Signal Process.*, vol. 140, no. 6, pp. 362–370, Dec. 1993.
- [25] T. S. Rappaport, *Wireless Communications: Principles and Practice*, 2nd ed. Englewood Cliffs, NJ: Prentice-Hall, 1996.
- [26] P. Chevalier, L. Albera, P. Comon, and A. Ferréol, "Comparative performance analysis of eight blind source separation methods on radiocommunications signals," *Proc. IEEE IJCNN*, vol. 1, pp. 273–278, 2004.
- [27] J. L. Lacoume, P. O. Amblard, and P. Comon, *Statistiques D'Ordre Supérieur Pour la Traitement du Signal*. Paris, France: Masson, 1997.
- [28] M. Souden, S. Affes, and J. Benesty, "A new approach to blind separation of two sources with three sensors," *Proc. IEEE 64th VTC*, pp. 1–5, 2006.
- [29] P. Stoica and A. Nehorai, "MUSIC, maximum likelihood, and Cramer-Rao bound: further results and comparisons," *IEEE Trans. Acoust., Speech, Signal Process.*, vol. 38, pp. 2140–2150, Dec. 1990.
- [30] J. P. Delmas and H. Abeida, "Cramer-Rao bounds of DOA estimates for BPSK and QPSK modulated signals," *IEEE Trans. Signal Process.*, vol. 54, no. 1, pp. 117–126, Jan. 2006.
- [31] M. Souden, S. Affes, and J. Benesty, "A two-stage approach to localize spatially distributed sources," *Proc. IEEE ISSPA*, 2007, invited paper.
- [32] P. Chargé, Y. Wang, and J. Saillard, "A non-circular sources direction finding method using polynomial rooting," *Signal Process.*, vol. 81, no. 8, pp. 1765–1770, Aug. 2001.
- [33] H. Abeida and J. P. Delmas, "MUSIC-like estimation of direction of arrival for non-circular sources," *IEEE Trans. Signal Process.*, vol. 54, no. 7, pp. 2678–2690, Jul. 2006.
- [34] B. Ottersten, P. Stoica, and R. Roy, "Covariance matching estimation techniques for array signal processing application," *Signal Process.*, vol. 8, no. 3, pp. 185–210, Jul. 1998.
- [35] S. M. Kay, *Fundamentals of Statistical Signal Processing I: Estimation Theory*. Englewood Cliffs, NJ: Prentice-Hall, 1993.



Mehrez Souden (S'06) was born in 1980. He received the Diplôme d'Ingénieur in Signals and Systems (with Honors) from the École Polytechnique de Tunisie and the M.Sc. degree in telecommunications from the Institut National de la Recherche Scientifique-Énergie, Matériaux, et Télécommunications (INRS-ÉMT), Université du Québec, Montréal, QC, Canada, in 2004 and 2006, respectively.

Since January 2006, he has been pursuing the Ph.D. degree in telecommunications engineering at the INRS-ÉMT. His research focuses on antenna and microphone array processing with an emphasis on source localization and noise reduction for wireless communications and acoustics applications.

Mr. Souden is the recipient of the National grant from the Tunisian Government.



Sofiène Affès (S'94–M'95–SM'04) received the Diplôme d'Ingénieur in electrical engineering in 1992, and the Ph.D. degree with honors in signal processing in 1995, both from the École Nationale Supérieure des Télécommunications (ENST), Paris, France.

He has been with INRS-EMT, University of Quebec, Montreal, Canada, first as a Research Associate (1995 to 1997), then as an Assistant Professor until 2000. Currently, he is an Associate Professor in the Wireless Communications Group.

His research interests are in wireless communications, statistical signal and array processing, adaptive space-time processing and MIMO. From 1998 to 2002, he was leading the radio-design and signal processing activities of the Bell/Nortel/NSERC Industrial Research Chair in Personal Communications at INRS-EMT, Montreal, Canada. Currently, he is actively involved in a major project in wireless of Partnerships for Research on Microelectronics, Photonics and Telecommunications (PROMPT-Quebec).

Professor Affès is the corecipient of the 2002 Prize for Research Excellence of INRS and currently holds a Canada Research Chair in Wireless Communications. He served as a General Co-Chair of the IEEE VTC'2006-Fall conference, Montreal, and currently acts as a member of Editorial Board of the *Wiley Journal on Wireless Communications and Mobile Computing* and of the IEEE TRANSACTIONS ON WIRELESS COMMUNICATIONS.



Jacob Benesty (M'98–SM'04) was born in 1963. He received the Master's degree in microwaves from Pierre and Marie Curie University, France, in 1987, and the Ph.D. degree in control and signal processing from Orsay University, France, in April 1991. During his Ph.D. program (from November 1989 to April 1991), he worked on adaptive filters and fast algorithms at the Centre National d'Études des Télécommunications (CNET), Paris, France.

From January 1994 to July 1995, he was with Telecom Paris University working on multichannel

adaptive filters and acoustic echo cancellation. From October 1995 to May 2003, he was first a Consultant and then a Member of the Technical Staff at Bell Laboratories, Murray Hill, NJ. In May 2003, he joined the University of Quebec, INRS-EMT, Montreal, Quebec, Canada, as an Associate Professor. His research interests are in signal processing, acoustic signal processing, and multimedia communications. He coauthored the books *Acoustic MIMO Signal Processing* (Berlin: Springer-Verlag, 2006) and *Advances in Network and Acoustic Echo Cancellation* (Berlin: Springer-Verlag, 2001). He is also a coeditor/coauthor of the books *Speech Enhancement* (Berlin: Springer-Verlag, 2005), *Audio Signal Processing for Next Generation Multimedia Communication Systems* (Boston, MA: Kluwer Academic, 2004), *Adaptive Signal Processing: Applications to Real-World Problems* (Berlin: Springer-Verlag, 2003), and *Acoustic Signal Processing for Telecommunication* (Boston, MA: Kluwer Academic, 2000).

Dr. Benesty received the 2001 Best Paper Award from the IEEE Signal Processing Society. He was a member of the editorial board of the *EURASIP Journal on Applied Signal Processing* and was the Co-Chair of the 1999 International Workshop on Acoustic Echo and Noise Control.